Hindawi
Journal of Immunology Research
Volume 2020, Article ID 7207354, 12 pages
https://doi.org/10.1155/2020/7207354

Research Article

Anti-Inflammatory Activity of Diterpenoids from *Celastrus orbiculatus* in Lipopolysaccharide-Stimulated RAW264.7 Cells

Hyun-Jae Jang,[1] **Kang-Hoon Kim**,[1] **Eun-Jae Park**,[1,2] **Jeong A. Kang**,[1,2] **Bong-Sik Yun**,[2] **Seung-Jae Lee**,[1] **Chan Sun Park**,[1] **Soyoung Lee**,[1] **Seung Woong Lee**,[1] **and Mun-Chual Rho**[1]

[1]*Immunoregulatory Materials Research Center, Korea Research Institute of Bioscience and Biotechnology, 181 Ipsin-gil, Jeongeup-si, Jeonbuk 56212, Republic of Korea*
[2]*Division of Biotechnology and Advanced Institute of Environment and Bioscience, College of Environmental and Bioresource Sciences, Jeonbuk National University, Iksan-si, Republic of Korea*

Correspondence should be addressed to Seung Woong Lee; lswdoc@kribb.re.kr and Mun-Chual Rho; rho-m@kribb.re.kr

Hyun-Jae Jang and Kang-Hoon Kim contributed equally to this work.

Received 26 December 2019; Revised 29 April 2020; Accepted 7 May 2020; Published 30 July 2020

Academic Editor: Qiang Zhang

Celastrus orbiculatus Thunb has been known as an ethnopharmacological medicinal plant for antitumor, anti-inflammatory, and analgesic effects. Although various pharmacological studies of *C. orbiculatus* extract has been reported, an anti-inflammatory mechanism study of their phytochemical constituents has not been fully elucidated. In this study, compounds **1**–**17**, including undescribed podocarpane-type trinorditerpenoid (**3**), were purified from *C. orbiculatus* and their chemical structure were determined by high-resolution electrospray ionization mass (HRESIMS) and nuclear magnetic resonance (NMR) spectroscopic data. To investigate the anti-inflammatory activity of compounds **1**–**17**, nitric oxide (NO) secretion was evaluated in LPS-treated murine macrophages, RAW264.7 cells. Among compounds **1**–**17**, deoxynimbidiol (**1**) and new trinorditerpenoid (**3**) showed the most potent inhibitory effects (IC_{50}: 4.9 and 12.6 μM, respectively) on lipopolysaccharide- (LPS-) stimulated NO releases as well as proinflammatory mediators, such as inducible nitric oxide (iNOS), cyclooxygenase- (COX-) 2, interleukin- (IL-) 1β, IL-6, and tumor necrosis factor- (TNF-) α. Its inhibitory activity of proinflammatory mediators is contributed by suppressing the activation of nuclear transcription factor- (NF-) κB and mitogen-activated protein kinase (MAPK) signaling cascades including p65, inhibition of NF-κB (IκB), extracellular signal-regulated kinase (ERK), c-Jun NH_2-terminal kinase (JNK), and p38. Therefore, these results demonstrated that diterpenoids **1** and **3** obtained from *C. orbiculatus* may be considered a potential candidate for the treatment of inflammatory diseases.

1. Introduction

Celastrus orbiculatus Thunb. (Oriental bittersweet) is a perennial woody vine belonging to the family Celastraceae, which is native to East Asia including China, Japan, and Korea [1, 2]. *C. orbiculatus* has been traditionally prescribed as a herbal remedy for bacterial infection, insecticidal, and rheumatoid arthritis [3, 4]. Previous pharmacological studies has shown that these extracts containing diverse phytochemical components such as sesquiterpenoids, diterpenoids, triterpenoids, alkaloids, flavonoids, and phenolic compounds [5–10] exhibit various biological activity such as antitumor [11–14], antioxidant [9], antinociceptive [15], antiatherosclerosis [16], neuroprotective [17], and anti-inflammatory [18] effects. Although a variety of biological activities of *C. orbiculatus* extracts reported in the literatures, whether any phytochemical component contributes to their biological mechanisms other than celastrol, which is the main triterpenoid compound of *C. orbiculatus* [19, 20], has been discussed limitedly so far.

The major function of the inflammation is to defend the host from infectious pathogens and repair tissue injury through the action of leukocytes including macrophages, neutrophils, and lymphocytes [21, 22]. However, immoderate or prolonged inflammation contribute to the development of chronic inflammation diseases such as arthritis, asthma, Crohn's, and inflammatory bowel disease (IBD), resulting in swelling, pain, and eventually damage of tissue or organ dysfunction [23, 24]. Macrophage activated by antigen, pathogens, and endogenous inflammatory stimuli is associated with functional and physiological changes in the cells and generates proinflammatory and cytotoxic mediators such as nitric oxide (NO), tumor necrosis factor α (TNF-α), interleukin-1β (IL-1β), IL-6, reactive oxygen mediators, and hydrolytic enzymes [25, 26]. Excessive NO and inflammatory cytokines released from macrophages are implicated in cytotoxicity by initiating both apoptosis and necrosis of normal tissues as well as destruction of tumor cells and exogenous pathogens [27, 28]. Thus, blocking these inflammatory mediators is considered to be effective for prevention of inflammation diseases.

Binding of these inflammatory mediators or bacterial lipopolysaccharide (LPS) to specific receptors including Toll-like receptors (TLRs) lead to the inflammatory responses, through the transmembrane signal transduction and intracellular responses such as nuclear transcription factor-κB (NF-κB) and mitogen-activated protein kinases (MAPKs) [29, 30]. The activation of NF-κB is involved in the phosphorylation of IκB, resulting in the release of NF-κB into the nucleus, which functions as a transcription factor for expressing proinflammatory target genes including inducible nitric oxide synthesis (iNOS), cyclooxygenase 2 (COX-2), TNF-α, IL-1β, and IL-6 [31]. Extracellular signal-regulated kinase (ERK), c-Jun NH_2-terminal kinase (JNK), and p38 kinase are generally known as subfamilies of MAPKs, and this phosphorylation involved in NF-κB activation modulates proinflammation mediators, such as iNOS and COX-2 in activated macrophages [23, 32, 33]. Therefore, the development of natural sources targeting the NF-κB and MAPK cascades can be a potential therapeutic for inflammatory diseases.

In current study, the chemical structures of phytochemical constituents (**1**–**17**) isolated from *C. orbiculatus* were determined by spectroscopic data including NMR and ESI-MS. Among components obtained from *C. orbiculatus*, compounds **1** and **3**, both of which are podocarpane trinorditerpenoids, exhibited most potent inhibitory activity against LPS-treated NO release, and their anti-inflammatory activity was explored through underlying molecular mechanisms including NF-κB and MAPK signaling pathway.

2. Materials and Methods

2.1. General Experimental Procedures. Column chromatography was performed with silica gel (Kieselgel 60, 230-400 mesh, Merck, Darmstadt, Germany), and silica gel 60 F_{254} and RP-18 F_{254}s (Merck) were used for TLC analysis. Medium-pressure liquid chromatography (MPLC) was performed using a Combiflash RF (Teledyne Isco, Lincoln, NE, USA), and semipreparative HPLC was performed on a Shimadzu LC-6 AD (Shimadzu Co., Tokyo, Japan) instrument equipped with a SPD-20A detector using Phenomenex Luna C_{18} (250 × 21.2 mm, 5 μm, Phenomenex, Torrance, CA, USA), Phenomenex Kinetex C_{18} (150 × 21.2 mm, 5 μm), Phenomenex Luna C_8 (150 × 21.2 mm, 5 μm), and YMC C_{18} J'sphere ODS H80 (250 × 20 mm, 4 μm, YMC Co., Kyoto, Japan) columns. ^{1}H-, ^{13}C-, and 2D NMR spectroscopic data were measured on a JEOL JNM-ECA600 or JEOL JNM-EX400 instrument (JEOL, Tokyo, Japan) using TMS as a reference. Optical rotation was recorded on a JASCO P-2000 polarimeter (Jasco Co., Tokyo, Japan). UV spectrum was obtained using SpectraMax M_2^e spectrophotometer (Molecular Devices, Sunnyvale, CA, USA). IR data were acquired using a Spectrum Jas.co FT/IR-4600 spectrometers (Jasco Corp., Tokyo, Japan). HRESIMS data were obtained using a Waters SYNAPT G2-Si HDMS spectrometer (Waters, Milford, MA, USA).

2.2. Plant Material. Celastrus orbiculatus (60 kg) was purchased from the Kyung-dong market in Seoul, Korea. One of the authors (M.C. Rho) performed botanical identification, and a voucher specimen (KRIB-KR2016-052) was deposited at the laboratory of the Immunoregulatory Materials Research Center, Jeonbuk Branch of the KRIBB.

2.3. Isolation of Compounds **1** *and* **3**. Pulverized stem of *Celastrus orbiculatus* (60 kg) was extracted at room temperature with 95% EtOH (200 L × 2), and the filtrate was concentrated *in vacuo* to afford the EtOH extract (1.5 kg). The EtOH extract (1.0 kg) was suspended in H_2O (2.0 L) and subsequently partitioned with *n*-hexane (COH, 225.3 g), EtOAc (COE, 164.9 g), and BuOH (114.4 g) fractions. The EtOAc-soluble extract (130 g) was chromatographed on a silica gel (silica gel, Fuji Silysia Chemical-Chromatorex, 130–200 mesh) column using a step gradient solvent system composed of $CHCl_3$ and MeOH (1 : 0 ⟶ 0 : 1, *v*/*v*) to give 17 fractions (COE1–COE17).

COE3 (2.6 g) was subjected to MPLC C_{18} column chromatography (130 g, H_2O : MeOH = 95 : 5 ⟶ 0 : 1, *v*/*v*) to generate 26 subfractions (COE3A–COE3Z). COE3Q (24 mg) was purified by semipreparative HPLC (Phenomenex Luna C_{18}, 250 × 21.2 mm, 5 μm, 65% MeCN, 6 mL/min) to obtain compound **1** (12.7 mg, t_R = 33.5 min).

COE5 (4.1 g) was chromatographed on a MPLC silica gel column (120 g, *n*-hexane : EtOAc, 1 : 0 → 0 : 1, *v*/*v*) to yield 15 sub-fractions (COE5A–COE5O), and COE5K (40 mg) was purified by semi-preparative HPLC (YMC, J'sphere ODS H80, 250 ×20 mm, 4 μm, 20% MeOH, 6 mL/min) to give compound **3** (3.4 mg, t_R =54.2 min). Compounds **2** and **4**–**17** were obtained from the hexane-soluble fraction using repeated column chromatography along with EtOAc-soluble fraction (Fig. S1).

Guaiacylglycerol-α, γ-*O*-nimbidiol diether (**3**) is a white amorphous powder with $[\alpha]_D^{25}$ −7 (*c* 0.1, CH_3OH); UV (CH_3OH) λ_{max} (log ε); 221 (4.26), 281 (2.90); IR (ATR) ν_{max} 3245, 2963, 2936, 2870, 1652, 1615, 1577, 1511, 1422, 1322, 1251, 1148, 1036, 947, 825 cm^{-1}; HRESIMS *m*/*z* 451.2116 $[M–H]^-$ (calcd. for $C_{27}H_{31}O_6^-$, 451.2126). For ^{1}H and ^{13}C NMR spectroscopic data, see Table 1 (Figs. S2–S16).

Table 1: ^{1}H and ^{13}C NMR spectroscopic data (δ ppm) for compound **3**.

Position	3		
	δ_C [a]		δ_H [b] (J in Hz)
1	39.2	CH_2	2.29, d (12.6)
			1.50, m
2	20.1	CH_2	1.83[a], m
			1.67, br d (13.8)
3	42.7	CH_2	1.55, d (13.2)
			1.32, td (13.2, 2.4)
4	34.3	C	—
5	51.4/51.3	CH	1.84[a], m
6	37.1/37.0	CH_2	2.64, m
7	200.5	C	—
8	126.2/126.1	C	—
9	153.0/152.9	C	—
10	39.4/39.3	C	—
11	113.4/113.3	CH	6.94[a], s/6.93[a], s
12	151.2/151.1	C	—
13	143.6/143.5	C	—
14	116.4	CH	7.54, s/7.52, s
15	33.2	CH_3	0.96[a], s/0.95[a], s
16	21.9	CH_3	1.03, s
17	23.9/23.8	CH_3	1.25[a], s/1.24[a], s
1'	129.0/128.9	C	—
2'	112.2/112.1	CH	7.00, d (1.8)
3'	149.4	C	—
4'	148.7	C	—
5'	116.5	CH	6.84, d (8.4)
6'	121.9	CH	6.90, dd (8.4, 1.8)
7'	78.7/78.6	CH	4.99, d (8.4)/4.97, d (8.4)
8'	80.0/79.9	CH	4.06, tdd (8.4, 4.2, 2.4)
9'	62.1	CH_2	3.71, ddd (12.6, 2.4, 1.2)
			3.47, ddd (12.6, 4.2, 1.8)
OCH_3-3'	56.6	CH_3	3.88, s/3.87, s

Assignments were done by HSQC, HMBC, and COSY experiments. Spectra were measured in methanol-d_4 at 600 and 150 MHz. [a]Overlapped signals.

2.4. Cell Culture. RAW264.7 (ATCC TIB-71) cells was cultured in Dulbecco's modified Eagle medium (DMEM) and RPMI 1640 medium supplemented with 10% fetal bovine serum, 2 mM glutamine, 100 U/mL penicillin, and 100 mg/mL streptomycin sulfate. Cells were maintained at 37°C in humidified air with 5% CO_2.

2.5. Measurement of NO Contents and Cell Cytotoxicity. NO assay was carried out for measurements of NO release using a previously reported method [34]. Briefly, RAW264.7 cells were plated at 1×10^5 cell density in 96-well microplate and cultured for 24 h. Compounds (**1**–**17**) were pretreated with increasing dose concentrations (0.5, 1, 5, 10, 25, 50, and 100 μM) and then stimulated with LPS (1 μg/mL, Sigma–Aldrich, St. Louis, MO, USA) for 18 h. The mixture of cell supernatant (100 μL) and Griess reagent (1% sulfanilamide +0.1% *N*-(1-naphthyl)ethylenediamine (Sigma–Aldrich, St. Louis, MO, USA)) in 5% phosphoric acid was recorded at 550 nm using a microplate reader (Varioskan LUX, Thermo Fisher Scientific Inc., Waltham, MA, USA). The percentage inhibition and logarithmic concentrations were presented as a graph using GraphPad Prism 5 (Fig. S16). IC_{50} values were calculated by nonlinear regression analysis as described previously [35]. RAW264.7 cell cytotoxicity was evaluated using 3-(4,5-dimethylthiazol-2-yl)-2,5-diphenyltetrazolium bromide (MTT) assay [34].

2.6. Immunoblot Analysis. The whole cell lysate were extracted using a Cell Lysis Buffer (Cell Signaling Technology, Beverly, MA, USA). Immunoblot analysis was performed using a previously described method [34]. After transfer to nitrocellulose (NC) membrane, the blocking membrane with 5% skimmed milk powder was incubated overnight at 4°C with primary antibody, including anti-phospho-JNK (1 : 1000), anti-JNK (1 : 1000), anti-phospho-p38 (1 : 1000), anti-p38 (1 : 1000), anti-phospho-ERK (1 : 1000), anti-ERK (1 : 1000), anti-phospho-p65 (1 : 1000), anti-p65 (1 : 1000), anti-phospho-IκBα (1 : 1000), anti- IκBα (1 : 1000), anti-COX-2 (1 : 1000), anti-iNOS (1 : 1000), and anti-β-actin antibodies (Cell Signaling, Beverly, MA, USA). The membranes were then incubated with a horseradish peroxide-conjugated anti-rabbit secondary antibody (1 : 5000) at room temperature. The band densities were calculated with Quantity One software (Bio-Rad Laboratories, Hercules, CA, USA).

2.7. Real-Time PCR Using TaqMan Probe. Total RNA was extracted from RAW264.7 cells using the TaKaRa MiniBEST Universal RNA Extraction Kit following the manufacturer's instructions (Takara Bio Inc., Japan). The complementary DNA (cDNA) was synthesized from 1 μg of the total RNA using a PrimeScript 1st strand cDNA synthesis kit (Takara Bio Inc. Japan). Quantitative real-time PCR (qPCR) of IL-1bβ (Mm00434228_m1), IL-6 (Mm00446190_m1), and TNF (Mm00443258_m1) was performed with a TaqMan Gene Expression Assay Kit (Thermo Fisher Scientific, San Jose, CA, USA). To normalize the gene expression, an 18S rRNA endogenous control (Applied Biosystems, Foster City, CA, USA) was used. The qPCR was employed to verify the mRNA expression using a StepOnePlus Real-Time PCR System. To quantify mRNA expression, TaqMan mRNA assay was performed according to the manufacturer's protocol (Applied Biosystems). PCR amplification was analyzed using the comparative $^{\Delta\Delta CT}$ method.

2.8. Statistical Analysis. Half-maximal inhibitory concentration (IC_{50}) values expressed as 95% confidence intervals were calculated by nonlinear regression analysis using GraphPad Prism 5 software (GraphPad software, San Diego, CA, USA). Each experiment, including immunoblot and real-time PCR, was performed independently three times, and these data represent the mean ± SEM. The statistical significance of each value was measured by the unpaired Student t-test. $^{*}p < 0.05$, $^{**}p < 0.01$, and $^{***}p < 0.001$ were considered significant.

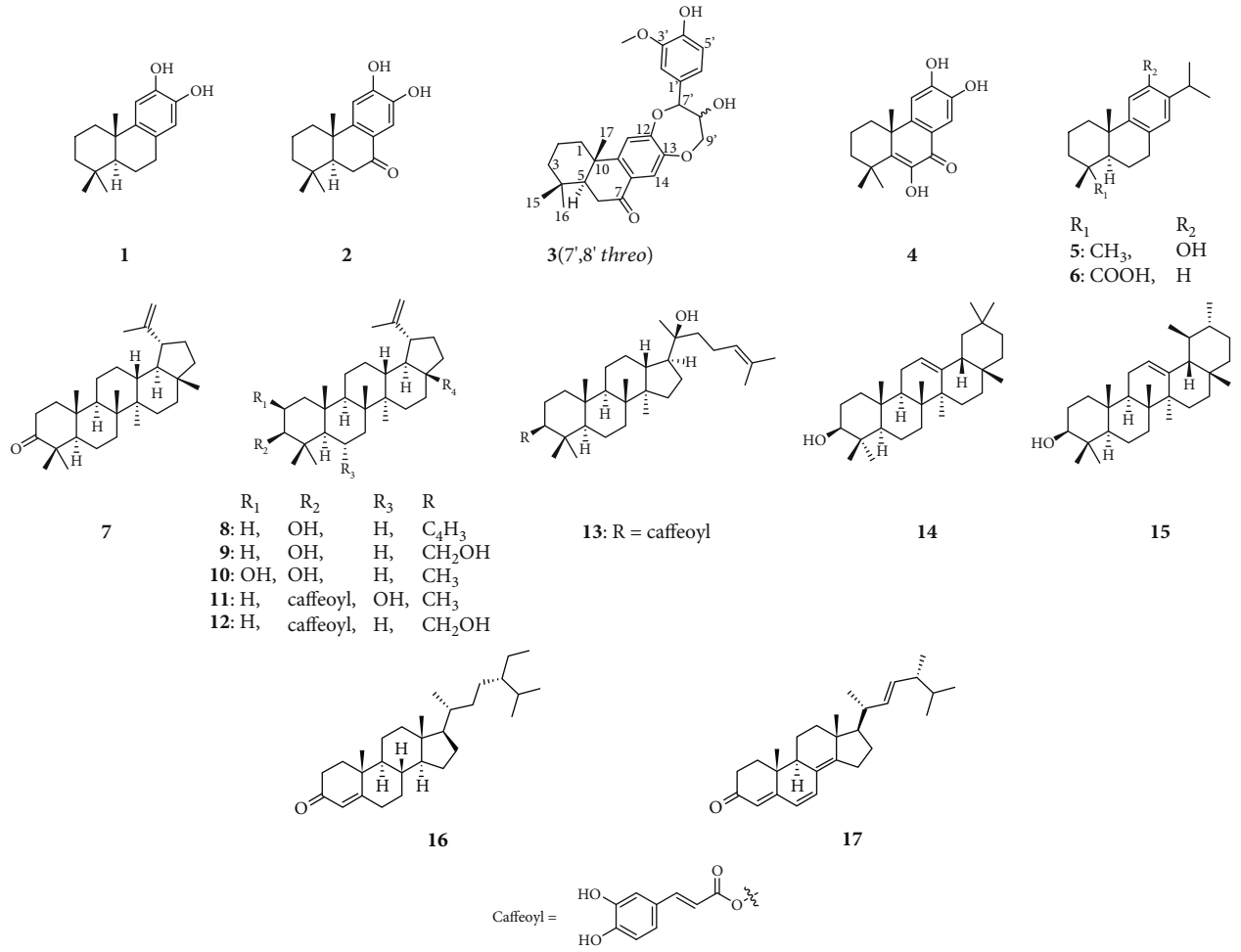

Figure 1: Chemical structure of compounds **1**–**17**.

3. Results and Discussion

Although *C. orbiculatus* is regarded as a medicinal plant including several terpenoids in East Asia and is treated with clinical prescription for health management [11, 36, 37], the biological activity and its composition against the inflammatory action of *C. orbiculatus* have hardly been found. In our search for novel anti-inflammatory agents from *C. orbiculatus*, the *n*-hexane and ethyl acetate-soluble fractions of *C. orbiculatus* were isolated to yield six diterpenoids (**1**–**6**), nine triterpenoids (**7**–**15**), and two steroids (**16** and **17**) using various column chromatography. Their chemical structures were elucidated as (+)-7-deoxynimbidiol (**1**) [38], nimbidiol (**2**) [39], celaphanol A (**4**) [39], (+)-ferruginol (**5**) [40], dehydroabietic acid (**6**) [41], lupenone (**7**) [42], lupeol (**8**) [42], betulin (**9**) [43], 2β,3β-dihydroxylup-20(29)-ene (**10**) [44], 3β-caffeoyloxylup-20(29)-en-6α-ol (**11**) [45], lup-20(29)-en-28-ol-3β-yl caffeate (**12**) [43], dammarenediol II 3-caffeate (**13**) [46], β-amyrin (**14**) [47], α-amyrin (**15**) [47], sitostenon (**16**) [48], and ergone (**17**) [49], compared to previous reported spectroscopic data, NMR, MS, and optical rotation values. Among these, 13 compounds (**3**, **5**–**13**, and **15**–**17**) containing compound 3 determined as novel podocarpane trinorditerpenoid based on HRESIMS and NMR data were first reported from *C. orbiculatus* (Figs. S2–S16). The scheme for the isolation of compounds from *Celastrus orbiculatus* was exhibited (Fig. S1).

Compound **3** was obtained as white amorphous powder, and its molecular weight of $C_{27}H_{32}O_6$ was determined by HRESIMS deprotonated molecular ion $[M–H]^-$ at *m*/*z* 451.2116 (calcd. 451.2126) (Fig. S2). The IR spectrum showed a hydroxy, carbonyl group, and aromatic ring absorption bands (3245, 1652, 1615, 1577, 1511, and 1422 cm^{-1}) (Fig. S3). The ^1H NMR spectrum displayed three methyl protons (δ_H 0.96/0.95 (s, H_3-15), 1.03 (s, H_3-16), and 1.25/1.24 (s, H_3-17)), two aromatic protons (δ_H 7.54/7.52 (s, H-14), 6.94/6.93 (s, H-11)), 1,3,4-trisubstituted aromatic ring protons (δ_H 7.00 (d, J = 1.8 Hz, H-2′), 6.84 (d, J = 8.4 Hz, H-5′), 6.90 (dd, J = 8.4, 1.8 Hz, H-6′)), two oxymethine protons (δ_H 4.99/4.97 (d, J = 8.4 Hz, H-7′), 4.06, (m, H-8′)), one oxymethylene proton (δ_H 3.71 (dq, J = 12.6, 1.2 Hz, H-9′a), 3.47 (dq, J = 12.6, 1.8 Hz, H-9′b)), and one methoxy proton (δ_H 3.88/3.87 (s, OCH_3-3′)) (Fig. S4). The ^{13}C and DEPT NMR spectroscopic data were indicated as the resonance for 27 carbons, including 12 aromatic ring carbons (δ_C 126.2/126.1

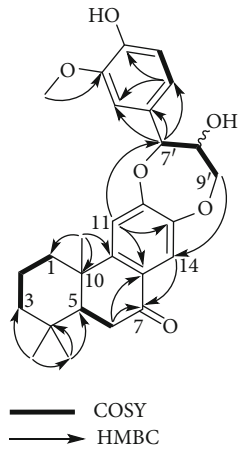

Figure 2: Key COSY and HBMC correlations for compound **3**.

(C-8), 153.0/152.9 (C-9), 113.4/113.3 (C-11), 151.2/151.1 (C-12), 143.6/143.5 (C-13), 116.4 (C-14), 129.0/128.9 (C-1′), 112.2/112.1 (C-2′), 149.4 (C-3′), 148.7 (C-4′), 116.5 (C-5′), and 121.9 (C-6′)), three methyl carbons (δ_C 33.2 (C-15), 21.9 (C-16), and 23.9/23.8 (C-17)), four methylene carbons (δ_C 39.2 (C-1), 20.1 (C-2), 42.7 (C-3), 37.1/37.0 (C-6)), one oxymethylene carbon (δ_C 62.1 (C-9′)), one methine carbon (δ_C 51.4/51.3 (C-5)), two oxymethine carbons (δ_C 78.7/78.6 (C-7′), 80.0/79.9 (C-8′)), two quaternary carbons (δ_C 34.3 (C-4), 39.4/39.3 (C-10)), methoxy carbon (δ_C 56.6 (OCH_3-3′)), and carbonyl carbon (δ_C 200.5 (C-7)) (Fig. S4 and S5). Its 1D NMR data closely resembled that of nimbidiol (**2**), which is previously isolated from *Celastrus* genus [39], except for the additional guaiacylglycerol group based on key COSY (H-7′/H-8′/H_2-9′) and HMBC (H-7′/C-1′, -2′, -3′ and OCH_3-3/C-3′) correlations (Figs. S8 and S10). The positions of α and γ in the guaiacylglycerol group were determined to be located at OH-12 and OH-13 of nimbidiol moiety, respectively, which involved a diether moiety, on the basis of the long range correlations (HMBC) between H-11 and C-7′ (α) and between H_2-9 (γ) and C-14 (Figure 1 and Fig. S10). The relative configuration of **3** was elucidated to be the same as that of nimbidiol by NOESY correlation between H-5 and H_3-15 and between H_3-16/H_3-17. Furthermore, the large coupling constant for $J_{7'/8'}$ (8.4 Hz) in the guaiacylglycerol group and no observation of NOE correlation between H-7′ and H-8′ indicated relative *threo* configuration (Fig. S11). Therefore, a pair of 1D NMR spectra of the same pattern showed that ′ is a 1 : 1 mixture of *threo* isomers between C-7′ and -8′. The structure of **3** was elucidated as shown in Figure 2, named guaiacylglycerol-α, γ-*O*-nimbidiol diether.

In maintenance of homeostasis from various organs systems, NO has been recognized as one of the important biological mediator involved in the various pathophysiological and physiological mechanisms, such as neurotransmitters, host defense against pathogenic microorganism, and regulation of immune systems [50]. However, the overproduction of NO in intracellular levels is associated to inflammatory diseases and carcinogenesis, and measurement of NO content has been employed by various literatures on the anti-inflammatory properties of phytochemicals derived from natural products [51]. To investigate whether NO production stimulated by LPS was inhibited by phytochemicals isolated from *C. orbiculatus*, compounds **1**–**17** were tested by NO assay in the RAW264.7 cells. As shown in Table 2, **1**–**4**, **11**, and **12** showed potent inhibitory activity against LPS-treated NO secretion based on 50% inhibitory effect at 50 μM concentration compared to only LPS-treated control group (IC_{50}: 4.9–40.0 μM) (Fig. S17), and all isolates did not affect cytotoxicity at IC_{50} concentration, respectively (Fig. S18). Among isolates showing NO inhibitory effect, **1** and **3**, which are podocarpane-type trinorditerpenoid class, were selected to evaluate further anti-inflammatory activity at 5 or 10 μM concentrations, respectively, which are approximately IC_{50}values without cytotoxicity effect by compounds.

iNOS is a major downstream mediator of inflammation in several cell types including macrophage cells [52]. During the course of an inflammatory response, large amount of NO formed by the action of iNOS surpass the physiological amounts of NO [53], and consequentially, iNOS overproduction reflects the degree of inflammation [54, 55]. COX-2 is an inducible enzyme that has a role in the development of epithelial cell dysplasia, carcinoma, wound edge of tissue, and inflammatory diseases such as arthritis, allergic asthma, and atopic dermatitis [56–58]. The expression of COX-2 is a key mediator of inflammatory pathway, which is representatively the NF-κB signaling pathway [59, 60].

In order to examine the biological evidence of effectively reduced NO production after treatment with **1** and **3**, we performed the immunoblot analysis to investigate whether **1** and **3** suppressed the upregulation of iNOS and COX-2 protein expression after LPS-activated inflammation condition. As shown in Figure 3, **1** and **3** dose dependently inhibited iNOS and COX-2 protein expression on LPS-induced inflammation in RAW264.7 cells. In addition, a comparison of nitric oxide production between compound **1**, **3**, and celastrol was exhibited (Fig. S19).

Each protein expression level was represented as relative ratio values of iNOS/β-actin and COX-2/β-actin (Figures 3(c)

Table 2: Inhibitory effects of compounds (**1**–**17**) on LPS-induced NO production.

Compound	IC_{50} (μM)	Compound	IC_{50} (μM)
1	4.89 (4.77–5.01)	**10**	>50
2	38.72 (17.50–85.66)	**11**	18.07 (10.74–30.42)
3	12.60 (10.65–14.89)	**12**	39.99 (30.42–52.58)
4	13.13 (9.15–18.84)	**13**	>50
5	>50	**14**	>50
6	>50	**15**	>50
7	>50	**16**	>50
8	>50	**17**	>50
9	>50	**Dexamethasone**[a]	0.016 (0.011– 0.023)

The IC_{50} values are showed with 95% confidence intervals (95% CIs). [a]Cytotoxicity was not observed at the IC_{50} concentration. [b]Dexamethasone used as the positive control.

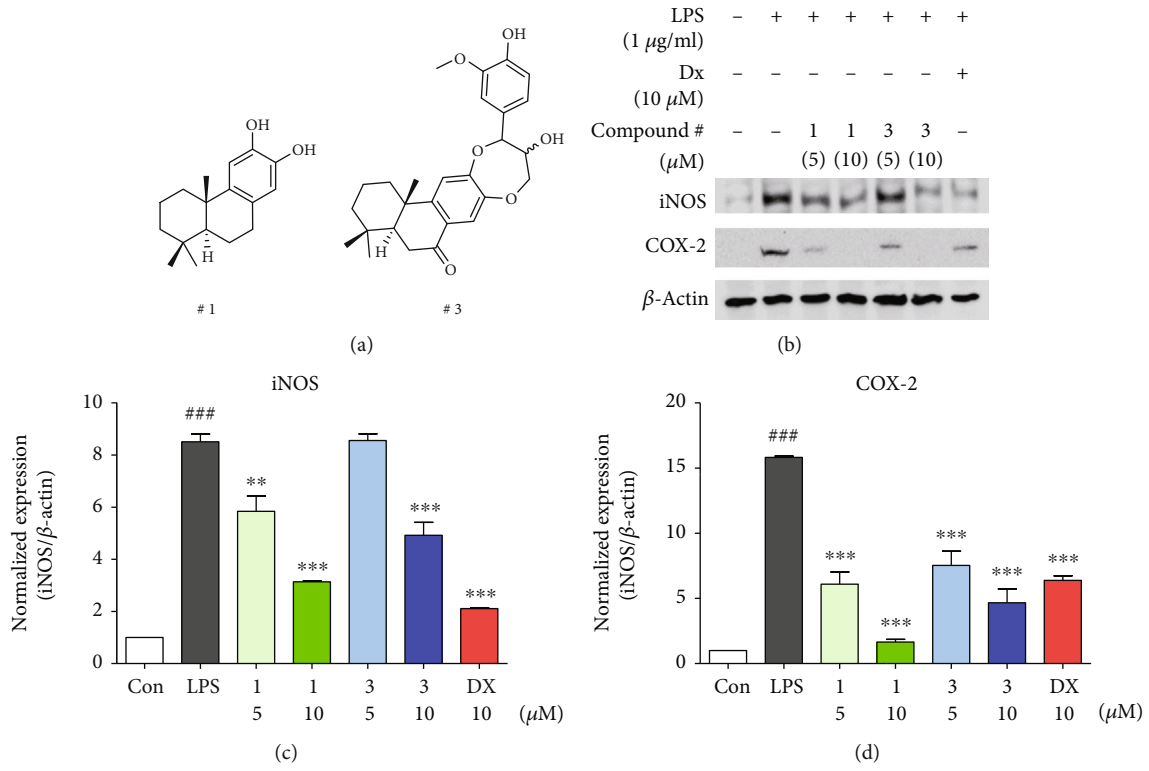

Figure 3: Compounds **1** and **3** showed anti-inflammatory effects through inhibiting iNOS and COX-2. (a) Chemical structure of compounds **1** and **3**. (b) Compounds **1** and **3** decreased iNOS and COX-2 protein expression levels in LPS-induced RAW264.7 cells. (c, d) Relative ratio of iNOS and COX-2 versus β-actin was measured using densitometry, and dexamethasone was used as positive control. These graphs represented that compounds **1** and **3** dose dependently inhibited iNOS and COX-2 levels in immunoblot analysis. Cells were pretreated with each compound for 2 h and stimulated with LPS (1 μg/mL) for 16 h. Immunoblot analysis performed a triplicate test, and results are expressed as means ± SEM. An unpaired Student t-test was used for statistical analysis. $^{###}p < 0.001$, $^{**}p < 0.01$, and $^{***}p < 0.001$ versus LPS.

and 3(d)). The fold-change values in iNOS and COX-2 expression in the presence of **1** and **3** was as follows: control (1 ± 0), LPS (8.51 ± 0.51/15.82 ± 0.15), **1** (5 μM: 5.84 ± 1.02 /6.08 ± 1.61 and 10 μM: 3.13 ± 0.05/1.65 ± 0.34), **3** (5 μM: 8.55 ± 0.44/7.53 ± 1.88 and 10 μM: 4.91 ± 0.86/4.66 ± 1.84), and dexamethasone (10 μM: 2.1 ± 0.06/6.38 ± 0.59). These results suggested that **1** and **3** prevented NO production via inhibition iNOS and COX-2 expression under LPS-induced inflammation condition in macrophages.

Dexamethasone or nonsteroidal anti-inflammatory drugs (NSAIDs) [61] are well known for blocking the MAPKs and NF-κB signaling cascades and results in potent anti-inflammatory activity through the reduction of proinflammatory mediators such as iNOS and COX-2. MAPK (JNK, ERK,

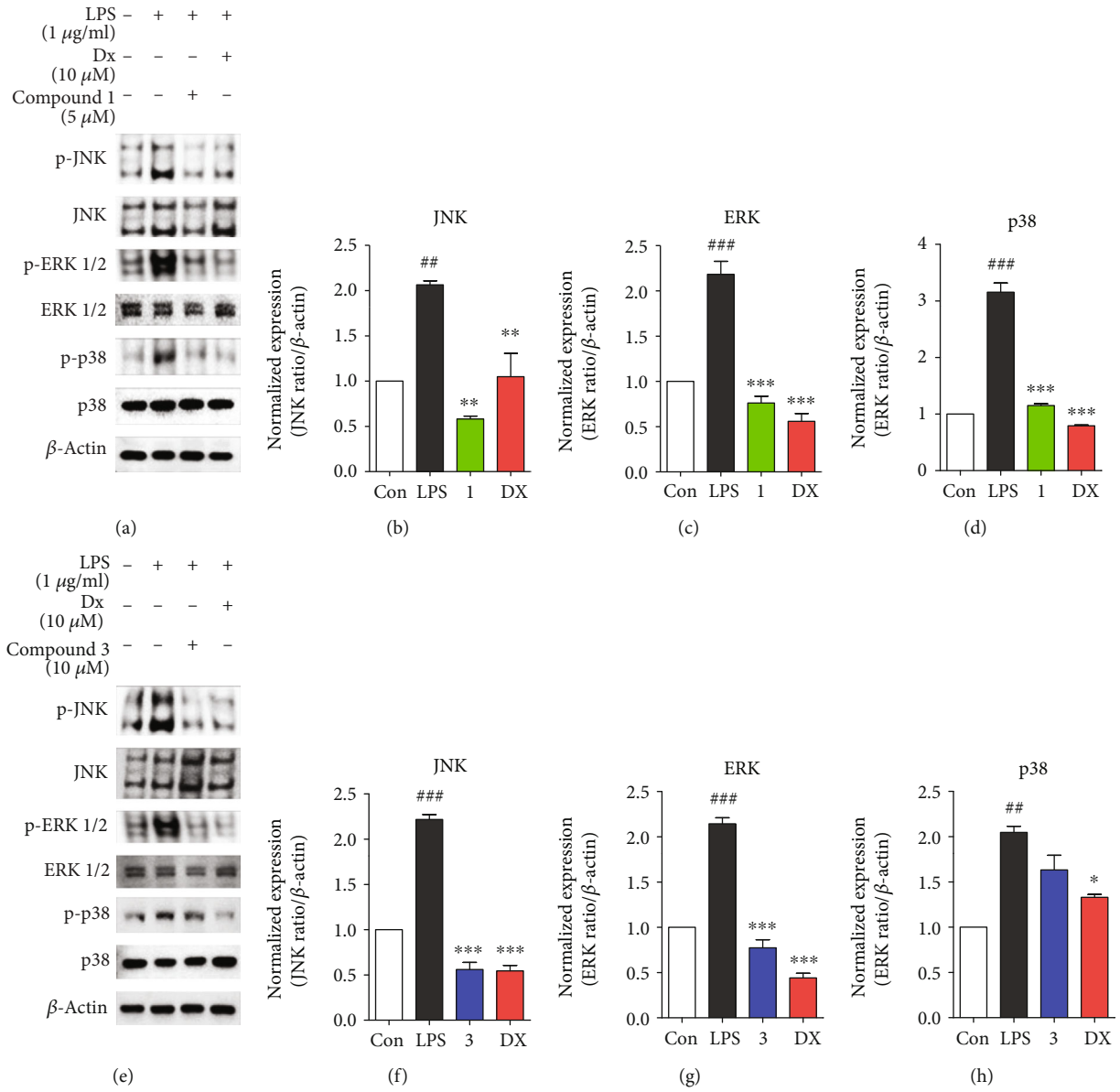

FIGURE 4: Compounds **1** and **3** suppressed MAPK signaling pathway. (a, e) Immunoblot analysis showed that phosphorylated protein levels of MAPK signaling cascades, JNK, ERK1/2, and p38 are inhibited by compounds **1** (a) and **3** (e) in RAW264.7 macrophages. (b–d, f–h) Total-JNK, ERK1/2, and p38 MAPK proteins were used as loading controls. (b, f) Cells were preincubated for 2 h with each compound **1** and **3** at concentrations of 5 and 10 μM, respectively, and stimulated with LPS (1 μg/mL) for 1 h. Dexamethasone served as the positive control. Immunoblot analysis performed triplicate experiments, and data represented means ± SEM. Significant difference was considered at the levels of $^{\#\#}p < 0.01$, $^{\#\#\#}p < 0.001$, $^{*}p < 0.05$, $^{**}p < 0.01$, and $^{***}p < 0.001$ versus LPS.

and p38) and NF-κB are crucial intracellular signaling pathways leading to the inflammatory response. These biological response are mediated by their transcription factors, such as activator protein- (AP-) 1, cAMP response element-binding protein (CREB), and NF-κB, which are phosphorylated and activated in the cytoplasmic or nuclear, resulting in an inflammatory action via the expression of target genes including pro-inflammatory cytokines IL-1β, IL-6, and TNF-α as well as iNOS and COX-2 proteins [62–64].

To further investigate anti-inflammatory effects associated with inhibition of NO production, iNOS, and COX-2, major inflammatory signaling cascades, MAPKs (JNK, ERK, and p38), and NF-κB, were evaluated with treatment of **1** or **3** in LPS-induced murine macrophages. As shown in Figures 4(a)–4(d), **1** remarkably inhibited phosphorylation of JNK (p-JNK), ERK (p-ERK), and p38 (p-p38) MAPK signaling molecules on LPS-activated inflammatory condition in RAW264.7 cells. Each protein expression level was presented as relative ratio values of p-JNK/JNK, p-ERK/ERK, and p-p38/p38. The fold-change values in p-JNK, p-ERK, and p-p38 expression in the presence of **1** were as follows: control (1 ± 0), LPS (2.06 ± 0.07/2.18 ± 0.24/3.15 ± 0.27), **1**

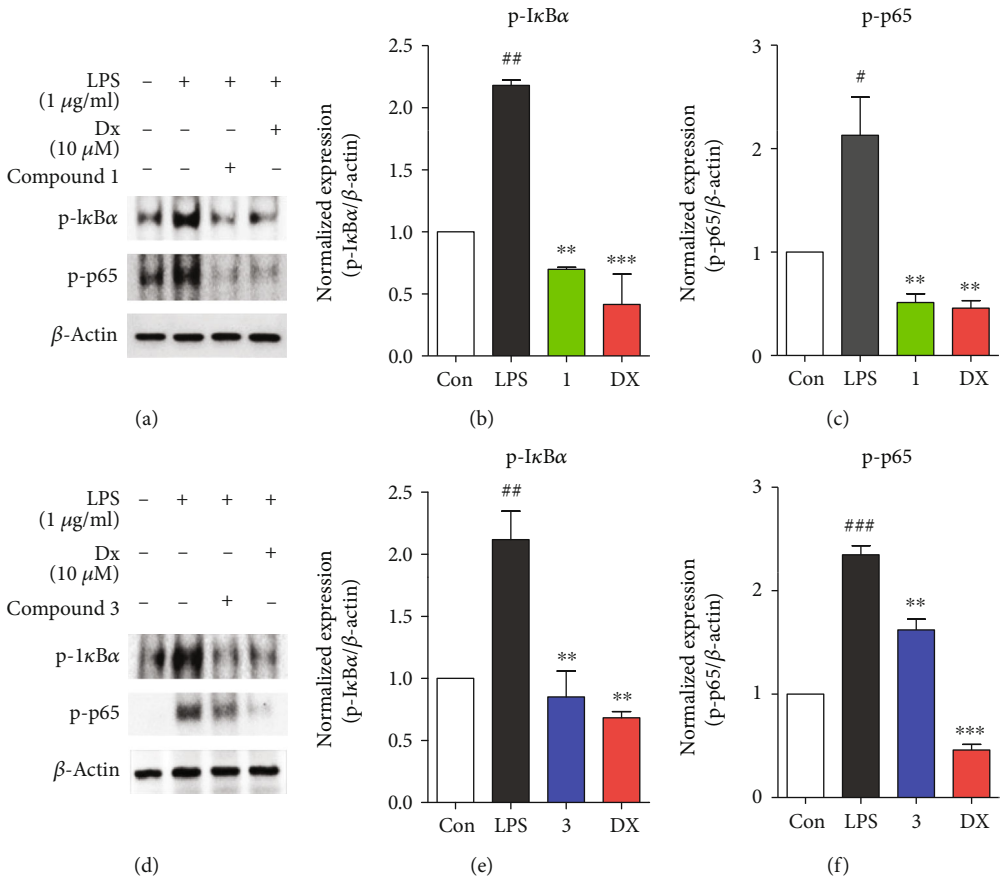

Figure 5: Compounds **1** and **3** attenuated the NF-κB signaling pathway. (a, d) Immunoblot analysis displayed that activation of the NF-κB signaling pathway was suppressed by compounds **1** (a) and **3** (d) in RAW264.7 cells. (b, c, e, f) The graph was expressed as the values of the relative ratio IκBα or p65 to β-actin protein expression level using densitometry. Cells were pretreated for 2 h with compounds **1** and **3** at concentrations of 5 and 10 μM, respectively, and stimulated with LPS (1 μg/mL) for 1 h. Dexamethasone was used as the positive control, and immunoblots analysis performed triplicate experiments. Values are means ± SEM, and an unpaired Student *t*-test was used for statistical analysis. $^{\#}p < 0.05$, $^{\#\#}p < 0.01$, $^{\#\#\#}p < 0.001$, $^{*}p < 0.05$, $^{**}p < 0.01$, and $^{***}p < 0.001$ represented significant differences from the LPS-treated group.

(5 μM: 0.58 ± 0.05/0.76 ± 0.12/1.14 ± 0.05), and dexamethasone (10 μM: 1.04 ± 0.44/0.55 ± 0.15/0.79 ± 0.02). As shown in Figures 4(e)–4(h), **3** markedly suppressed p-JNK and p-ERK, but not p-p38. The fold-change values in p-JNK, ERK, and p-p38 expression in the presence of **3** were as follows: control (1 ± 0), LPS (2.21 ± 0.09/2.14 ± 0.11/2.04 ± 0.11), **3** (10 μM: 0.56 ± 0.13/0.77 ± 0.15/1.63 ± 0.28), and dexamethasone (10 μM: 0.54 ± 0.05/0.44 ± 0.08/1.32 ± 0.05). Subsequently, immunoblot analysis was used to examine whether **1** and **3** affect the activation of NF-κB transcription factor through a decrease of phosphorylation of IκBα (p-IκBα) and p65 (p-p65). **1** and **3** significantly inhibited p-IκBα and p-p65, similar to the positive control, dexamethasone (Figure 5). Each protein expression level was expressed as relative ratio values of p-IκBα/β-actin and p-p65/β-actin as described in Figures 5(b), 5(c), 5(e), and 5(f). The fold-change values in p-IκBα and p-p65 expression in the presence of **1** were as follows: control (1 ± 0), LPS (2.17 ± 0.07/2.13 ± 0.63), **1** (5 μM: 0.69 ± 0.02/0.51 ± 0.14), and dexamethasone (10 μM: 0.41 ± 0.42/0.45 ± 0.12) (Figures 5(b) and 5(c)). The fold-change values in p-IκBα and p-p65 expression in the presence of **3** were as follows: control (1 ± 0), LPS (2.21 ± 0.09/2.34 ± 0.15), **3** (10 μM: 0.56 ± 0.13/1.62 ± 0.18), and dexamethasone (10 μM: 0.54 ± 0.05/0.45 ± 0.09) (Figure 5(e) and 5(f)). These results suggested that the anti-inflammatory activity of **1** and **3** is responsible for suppressing the MAPK and NF-κB signaling pathways.

The continuous overexpression of proinflammatory cytokines, IL-1β, IL-6, and TNF-α, is characterized as chronic inflammatory pathogenesis, which results in cell and tissue degeneration [63, 65], such as rheumatoid arthritis and inflammatory bowel diseases. Thus, following the hypothesis that these proinflammatory cytokines may be inhibited by **1** and **3**, we performed real-time PCR experiments to evaluate the inhibitory effect of IL-1β, IL-6, and TNF-α levels. In accordance with our hypothesis, **1** and **3** revealed a reduction in LPS-induced IL-1β, IL-6, and TNF-α gene expression at mRNA transcription levels (Figure 6). All taken together, these results indicated that the anti-inflammation activity of **1** and **3** was attributed

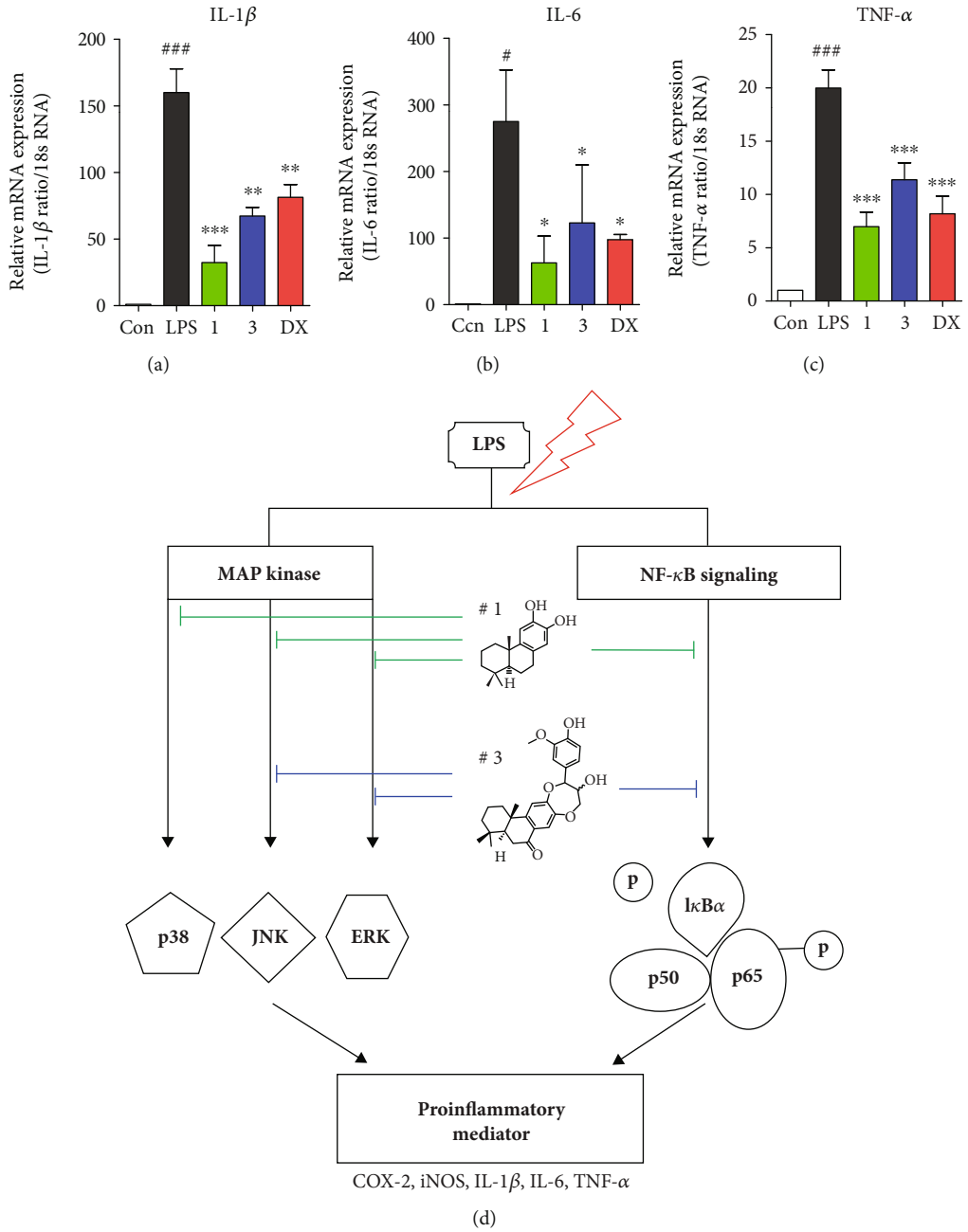

Figure 6: Compounds **1** and **3** downregulated proinflammatory mediators. (a–c) The mRNA expression levels of IL-1β, IL-6, and TNF-α were measured using quantitative real-time PCR experiment, and these proinflammatory cytokines were significantly diminished by compounds **1** and **3**. Cells were preincubated for 2 h with compounds **1** and **3** at concentration of 5 and 10 μM, respectively, and activated by LPS (1 μg/mL) for 2 h. Results represent as mean ± SEM, and dexamethasone was used as a positive control. $^{\#}p < 0.05$, $^{\#\#\#}p < 0.001$, $^{*}p < 0.05$, $^{**}p < 0.01$, and $^{***}p < 0.001$ indicated significant differences from the LPS-treated group. (d) Graphical depiction of the potent anti-inflammatory activity of compounds **1** and **3** in LPS-activated RAW264.7 cells by suppressing the MAPK and NF-κB signaling pathway.

to blockade of the MAPK and NF-κB signaling pathways via the suppression of p-ERK, p-JNK, p-p38, p-IκB, and p-p65 (Figure 6(d)).

4. Conclusion

In the present study, compounds **1**–**17** separated from *C. orbiculatus* using normal or reverse phase column chromatography were identified as six diterpenoids (**1**–**6**), nine triterpenoids (**7**–**15**), and two steroids (**16** and **17**) compared to previous reported spectroscopic data including NMR and MS. Of all isolates, 7-deoxynimbidiol (**1**) and novel podocarpane-type trinorditerpenoid (**3**) significantly exhibited the most significant inhibitory effects on LPS-activated proinflammatory mediator secretion, such as iNOS, COX-2, NO, IL-1β, IL-6, and TNF-α, and its anti-

inflammatory actions were exerted via downregulation of MAPK and NF-κB signaling cascade molecules including p-ERK, p-JNK, p-p38, p-IκB, and p-p65. Therefore, *C. orbiculatus* extract and its components **1** and **3** may be useful and safe treatments for inflammatory diseases such as rheumatoid arthritis, asthma, and atopic dermatitis, which can be applied to an alternative medical food in place of the conventional drugs, such as NSAIDs and dexamethasone.

Data Availability

The data used to support the findings of this study are available from the corresponding author upon request.

Conflicts of Interest

The authors have declared that there is no conflict of interest.

Authors' Contributions

Hyun-Jae Jang, Eun-Jae Park, Jeong A Kang, Seung Woong Lee, and Mun-Chual Rho performed the general experiments which were isolation and elucidation of chemical structures. Kang-Hoon Kim, Seung-Jae Lee, and Soyoung Lee carried out the biological experiments. Hyun-Jae Jang, Bong-Sik Yun, and Seung Woong Lee analyzed the spectroscopic data. Hyun-Jae Jang, Kang-Hoon Kim, and Seung Woong Lee wrote the manuscript. Hyun-Jae Jang and Kang-Hoon Kim contributed equally to this work.

Acknowledgments

This research was financially supported by the Agricultural Bio-Industry Technology Development Program of the Ministry of Agriculture, Food, and Rural Affairs (314011-5) and by a grant from the KRIBB Research Initiative Program (KGS1002012 and KGS1052012).

Supplementary Materials

Supplementary Figure 1: scheme for the isolation of compounds from Celastrus orbiculatus. Supplementary Figure 2: HRESIMS spectrum of **3**. Supplementary Figure 3: IR spectrum of **3**. Supplementary Figure 4: ^{1}H NMR (600 MHz, methanol-d4) spectrum of **3**. Supplementary Figure 5: ^{13}C NMR (150 MHz, methanol-d4) spectrum of **3**. Supplementary Figure 6: DEPT90 NMR (150 MHz, methanol-d4) spectrum of **3**. Supplementary Figure 7: DEPT-135 NMR (150 MHz, methanol-d4) spectrum of **3**. Supplementary Figure 8: COSY (600 MHz, methanold4) spectrum of **3**. Supplementary Figure 9: HMQC (600 MHz, methanol-d4) spectrum of **3**. Supplementary Figure 10: HMBC (600 MHz, methanol-d4) spectrum of **3**. Supplementary Figure 11: NOESY (600 MHz, methanol-d4) spectrum of **3**. Supplementary Figure 12: ^{1}H NMR (600 MHz, DMSO-d6) spectrum of **3**. Supplementary Figure 13: ^{13}C NMR (150 MHz, DMSOd6) spectrum of **3**. Supplementary Figure 14: COSY (600 MHz, DMSO-d6) spectrum of **3**. Supplementary Figure 15: HMQC (600 MHz, DMSO-d6) spectrum of **3**. Supplementary Figure 16: HMBC (600 MHz, DMSO-d4) spectrum of **3**. Supplementary Figure 17: inhibition percentage curves for the compounds **1**–**4**, **11**, and **12**. Supplementary Figure 18: cell viability 17 for the compounds **1**–**4**, **11**, and **12**. Supplementary Figure 19: a comparison of Nitric oxide production between compounds **1**, **3**, and celastrol. *(Supplementary Materials)*

References

[1] T. J. Tibbetts and F. W. Ewers, "Root pressure and specific conductivity in temperate lianas: exotic Celastrus orbiculatus (Celastraceae) vs. native Vitis riparia (Vitaceae)," *American Journal of Botany*, vol. 87, no. 9, pp. 1272–1278, 2000.

[2] S. Wu, C. Sun, K. Wang, and Y. Pan, "Preparative isolation and purification of celastrol from Celastrus orbiculatus Thunb. by a new counter-current chromatography method with an upright coil planet centrifuge," *Journal of Chromatography A*, vol. 1028, no. 1, pp. 171–174, 2004.

[3] B. S. Jung and M. K. Shin, "Encyclopedia of Illustrated Korean Natural Drugs," in *Encyclopedia of Illustrated Korean Natural Drugs*, p. 366, Young Lim Sa, Seoul, 1989.

[4] M. Wang, Q. Zhang, Q. Ren et al., "Isolation and characterization of sesquiterpenes fromCelastrus orbiculatusand their antifungal activities against phytopathogenic fungi," *Journal of Agricultural and Food Chemistry*, vol. 62, no. 45, pp. 10945–10953, 2014.

[5] H. Z. Jin, B. Y. Hwang, H. S. Kim, J. H. Lee, Y. H. Kim, and J. J. Lee, "Antiinflammatory constituents ofCelastrusorbiculatusInhibit the NF-κB activation and NO production," *Journal of Natural Products*, vol. 65, no. 1, pp. 89–91, 2002.

[6] L. I. Jian-Juan, J. YANG, L. Ü. Fang et al., "Chemical constituents from the stems of *Celastrus orbiculatus*," *Chinese Journal of Natural Medicines*, vol. 10, no. 4, pp. 279–283, 2012.

[7] J. Wu, Y. Zhou, L. Wang, J. Zuo, and W. Zhao, "Terpenoids from root bark of Celastrus orbiculatus," *Phytochemistry*, vol. 75, pp. 159–168, 2012.

[8] Y. Guo, X. Li, J. Wang, J. Xu, and N. Li, "A new alkaloid from the fruits of Celastrus orbiculatus," *Fitoterapia*, vol. 76, no. 2, pp. 273–275, 2005.

[9] B. Y. Hwang, H. S. Kim, J. H. Lee et al., "Antioxidant Benzoylated Flavan-3-ol Glycoside fromCelastrusorbiculatus," *Journal of Natural Products*, vol. 64, no. 1, pp. 82–84, 2001.

[10] K. Min, B. Hwang, H.-S. Lim et al., "(–)-Epiafzelechin: cyclooxygenase-1 inhibitor and anti-inflammatory agent from aerial parts ofCelastrus orbiculatus," *Planta Medica*, vol. 65, no. 5, pp. 460–462, 1999.

[11] H. Wang, L. Tao, T. Ni et al., "Anticancer efficacy of the ethyl acetate extract from the traditional Chinese medicine herb _Celastrus orbiculatus_ against human gastric cancer," *Journal of Ethnopharmacology*, vol. 205, no. 9, pp. 147–157, 2017.

[12] Y. Qian, T. Yang, X. Zhao et al., "Celastrus orbiculatus extracts induce apoptosis in mTOR-overexpressed human hepatocellular carcinoma HepG2 cells," *BMC Complementary and Alternative Medicine*, vol. 18, no. 1, p. 328, 2018.

[13] H. Jeon, "Anti-metastatic effects of celastrus orbiculatus extract in B16F10 melanoma cells," *Natural Product Sciences*, vol. 17, no. 2, pp. 135–141, 2011.

[14] L. Yang, Y. Liu, M. Wang et al., "Celastrus orbiculatus extract triggers apoptosis and autophagy via PI3K/Akt/mTOR

inhibition in human colorectal cancer cells," *Oncology Letters*, vol. 12, no. 5, pp. 3771–3778, 2016.

[15] H. J. Park, D. S. Cha, and H. Jeon, "Antinociceptive and hypnotic properties of _Celastrus orbiculatus_," *Journal of Ethnopharmacology*, vol. 137, no. 3, pp. 1240–1244, 2011.

[16] Y. Zhang, Y. Si, S. Yao et al., "Celastrus orbiculatus thunb. decreases athero-susceptibility in lipoproteins and the aorta of Guinea pigs fed high fat diet," *Lipids*, vol. 48, no. 6, pp. 619–631, 2013.

[17] X. J. Wang, L. Y. Wang, Y. Fu et al., "Promising effects on ameliorating mitochondrial function and enhancing Akt signaling in SH-SY5Y cells by (M)-bicelaphanol A, a novel dimeric podocarpane type trinorditerpene isolated from Celastrus orbiculatus," *Phytomedicine*, vol. 20, no. 12, pp. 1064–1070, 2013.

[18] Y. Lu, W. Zheng, S. Lin et al., "Identification of an oleanane-type triterpene hedragonic acid as a novel farnesoid X receptor ligand with liver protective effects and anti-inflammatory activity," *Molecular Pharmacology*, vol. 93, no. 2, pp. 63–72, 2018.

[19] H. S. Yang, J. Y. Kim, J. H. Lee et al., "Celastrol isolated from Tripterygium regelii induces apoptosis through both caspase-dependent and -independent pathways in human breast cancer cells," *Food and Chemical Toxicology*, vol. 49, no. 2, pp. 527–532, 2011.

[20] R. Cascão, J. E. Fonseca, and L. F. Moita, "Celastrol: A Spectrum of Treatment Opportunities in Chronic Diseases," *Frontiers in Medicine*, vol. 4, 2017.

[21] S.-J. Heo, J. Jang, B.-R. Ye et al., "Chromene suppresses the activation of inflammatory mediators in lipopolysaccharide-stimulated RAW 264.7 cells," *Food and Chemical Toxicology*, vol. 67, pp. 169–175, 2014.

[22] L. M. Coussens and Z. Werb, "Inflammation and cancer," *Nature*, vol. 420, no. 6917, pp. 860–867, 2002.

[23] K.-N. Kim, S.-J. Heo, W.-J. Yoon et al., "Fucoxanthin inhibits the inflammatory response by suppressing the activation of NF-κB and MAPKs in lipopolysaccharide-induced RAW 264.7 macrophages," *European Journal of Pharmacology*, vol. 649, no. 1–3, pp. 369–375, 2010.

[24] Y. P. Hwang, S. W. Jin, J. H. Choi et al., "Inhibitory effects of l-theanine on airway inflammation in ovalbumin-induced allergic asthma," *Food and Chemical Toxicology*, vol. 99, pp. 162–169, 2017.

[25] S. H. Yang, B. Le, V. P. Androutsopoulos et al., "Anti-inflammatory effects of soyasapogenol I-αa via downregulation of the MAPK signaling pathway in LPS-induced RAW 264.7 macrophages," *Food and Chemical Toxicology*, vol. 113, pp. 211–217, 2018.

[26] D. L. Laskin and J. D. Laskin, "Role of macrophages and inflammatory mediators in chemically induced toxicity," *Toxicology*, vol. 160, no. 1–3, pp. 111–118, 2001.

[27] J. W. Larrick and S. L. Kunkel, "The role of tumor necrosis factor and interleukin 1 in the immunoinflammatory response," *Pharmaceutical Research*, vol. 5, no. 3, pp. 129–139, 1988.

[28] J. W. Larrick and S. C. Wright, "Cytotoxic mechanism of tumor necrosis factor-α," *The FASEB Journal*, vol. 4, no. 14, pp. 3215–3223, 1990.

[29] J. L. Lai, Y. H. Liu, C. Liu et al., "Indirubin Inhibits LPS-Induced Inflammation via TLR4 Abrogation Mediated by the NF-kB and MAPK Signaling Pathways," *Inflammation*, vol. 40, no. 1, pp. 1–12, 2017.

[30] R. Qiu, W. Yao, H. Ji et al., "Dexmedetomidine restores septic renal function via promoting inflammation resolution in a rat sepsis model," *Life Sciences*, vol. 204, pp. 1–8, 2018.

[31] D. B. Reddy and P. Reddanna, "Chebulagic acid (CA) attenuates LPS-induced inflammation by suppressing NF-κB and MAPK activation in RAW 264.7 macrophages," *Biochemical and Biophysical Research Communications*, vol. 381, no. 1, pp. 112–117, 2009.

[32] S. J. Ajizian, B. K. English, and E. A. Meals, "Specific Inhibitors of p38 and Extracellular Signal-Regulated Kinase Mitogen-Activated Protein Kinase Pathways Block Inducible Nitric Oxide Synthase and Tumor Necrosis Factor Accumulation in Murine Macrophages Stimulated with Lipopolysaccharide and Interferon-γ," *The Journal of Infectious Diseases*, vol. 179, no. 4, pp. 939–944, 1999.

[33] H. Y. Zhou, E. M. Shin, L. Y. Guo et al., "Anti-inflammatory activity of 4-methoxyhonokiol is a function of the inhibition of iNOS and COX-2 expression in RAW 264.7 macrophages via NF-κB, JNK and p38 MAPK inactivation," *European Journal of Pharmacology*, vol. 586, no. 1–3, pp. 340–349, 2008.

[34] K. H. Kim, E. J. Park, H. J. Jang et al., "1-Carbomethoxy-β-Carboline, Derived from Portulaca oleracea L., Ameliorates LPS-Mediated Inflammatory Response Associated with MAPK Signaling and Nuclear Translocation of NF-κB," *Molecules*, vol. 24, no. 22, p. 4042, 2019.

[35] H.-J. Jang, E.-J. Park, S.-J. Lee et al., "Diarylheptanoids from Curcuma phaeocaulis suppress IL-6-induced STAT3 activation," *Planta Medica*, vol. 85, no. 2, pp. 94–102, 2019.

[36] M. Wang, X. Zhang, X. Xiong et al., "Efficacy of the Chinese traditional medicinal herb Celastrus orbiculatus Thunb on human hepatocellular carcinoma in an orthothopic fluorescent nude mouse model," *Anticancer Research*, vol. 32, no. 4, pp. 1213–1220, 2012.

[37] Y. Zhu, Y. Liu, Y. Qian et al., "Research on the efficacy of Celastrus Orbiculatus in suppressing TGF-β1-induced epithelial-mesenchymal transition by inhibiting HSP27 and TNF-α-induced NF-κB/Snail signaling pathway in human gastric adenocarcinoma," *BMC Complementary and Alternative Medicine*, vol. 14, no. 1, pp. 1–12, 2014.

[38] Y. Xiong, K. Wang, Y. Pan, H. Sun, and J. Tu, "Isolation, synthesis, and anti-tumor activities of a novel class of podocarpic diterpenes," *Bioorganic & Medicinal Chemistry Letters*, vol. 16, no. 4, pp. 786–789, 2006.

[39] B. Chen, H. Duan, and Y. Takaishi, "Triterpene caffeoyl esters and diterpenes from Celastrus stephanotifoli," *Phytochemistry*, vol. 51, no. 5, pp. 683–687, 1999.

[40] M. A. González and D. Pérez-Guaita, "Short syntheses of (+)-ferruginol from (+)-dehydroabietylamine," *Tetrahedron*, vol. 68, no. 47, pp. 9612–9615, 2012.

[41] T. A. Van Beek, F. W. Claassen, J. Dorado, M. Godejohann, R. Sierra-Alvarez, and J. B. P. A. Wijnberg, "Fungal biotransformation products of dehydroabietic acid," *Journal of Natural Products*, vol. 70, no. 2, pp. 154–159, 2007.

[42] V. S. P. Chaturvedula and I. Prakash, "Isolation and structural characterization of Lupane triterpenes from Polypodium vulgare," *Research Journal of Pharmaceutical Sciences*, vol. 1, no. 1, pp. 23–27, 2012.

[43] A. Patra, S. K. Chaudhuri, and S. K. Panda, "Betulin-3-caffeate from Quercus suber,13C-nmr spectra of some lupenes," *Journal of Natural Products*, vol. 51, no. 2, pp. 217–220, 1988.

[44] J. Huang, Z. H. Guo, P. Cheng, B. H. Sun, and H. Y. Gao, "Three new triterpenoids from Salacia hainanensis Chun et How showed effective anti-α-glucosidase activity," *Phytochemistry Letters*, vol. 5, no. 3, pp. 432–437, 2012.

[45] S. S. Awanchiri, H. Trinh-Van-Dufat, J. C. Shirri et al., "Triterpenoids with antimicrobial activity from Drypetes inaequalis," *Phytochemistry*, vol. 70, no. 3, pp. 419–423, 2009.

[46] Y. M. Ying, C. X. Zhang, K. M. Yu et al., "Chemical constituents of Celastrus rugosus," *Chemistry of Natural Compounds*, vol. 53, no. 3, pp. 589–591, 2017.

[47] I. Serbian and R. Csuk, "An improved scalable synthesis of α- and β-amyrin," *Molecules*, vol. 23, no. 7, p. 1552, 2018.

[48] J. Y. Chen, Y. F. Xie, T. X. Zhou, and G. W. Qin, "Chemical constituents of *Menispermum dauricum*," *Chinese Journal of Natural Medicines*, vol. 10, no. 4, pp. 292–294, 2012.

[49] H. C. Kwon, S. D. Zee, S. Y. Cho, S. U. Choi, and K. R. Lee, "Cytotoxic ergosterols frompaecilomyces sp. J300," *Archives of Pharmacal Research*, vol. 25, no. 6, pp. 851–855, 2002.

[50] F. Aktan, "iNOS-mediated nitric oxide production and its regulation," *Life Sciences*, vol. 75, no. 6, pp. 639–653, 2004.

[51] C. H. Kang, Y. H. Choi, S. Y. Park, and G. Y. Kim, "Anti-inflammatory effects of methanol extract of Codium fragile in lipopolysaccharide-stimulated RAW 264.7 cells," *Journal of Medicinal Food*, vol. 15, no. 1, pp. 44–50, 2012.

[52] P. Tripathi, P. Tripathi, L. Kashyap, and V. Singh, "The role of nitric oxide in inflammatory reactions," *FEMS Immunology & Medical Microbiology*, vol. 51, no. 3, pp. 443–452, 2007.

[53] Q. W. Xie, Y. Kashiwabara, and C. Nathan, "Role of transcription factor NF-kappa B/Rel in induction of nitric oxide synthase," *Journal of Biological Chemistry*, vol. 269, no. 7, pp. 4705–4708, 1994.

[54] K. S. Farley, L. F. Wang, H. M. Razavi et al., "Effects of macrophage inducible nitric oxide synthase in murine septic lung injury," *American Journal of Physiology-Lung Cellular and Molecular Physiology*, vol. 290, no. 6, pp. L1164–L1172, 2006.

[55] R. E. Sacco, W. R. Waters, K. M. Rudolph, and M. L. Drew, "Comparative nitric oxide production by LPS-stimulated monocyte-derived macrophages from Ovis canadensis and Ovis aries," *Comparative Immunology, Microbiology and Infectious Diseases*, vol. 29, no. 1, pp. 1–11, 2006.

[56] A. Futagami, M. Ishizaki, Y. Fukuda, S. Kawana, and N. Yamanaka, "Wound healing involves induction of cyclooxygenase-2 expression in rat skin," *Laboratory Investigation*, vol. 82, no. 11, pp. 1503–1513, 2002.

[57] E. Ricciotti and G. A. FitzGerald, "Prostaglandins and inflammation," *Arteriosclerosis, Thrombosis, and Vascular Biology*, vol. 31, no. 5, pp. 986–1000, 2011.

[58] C. S. Williams, M. Mann, and R. N. DuBois, "The role of cyclooxygenases in inflammation, cancer, and development," *Oncogene*, vol. 18, no. 55, pp. 7908–7916, 1999.

[59] S. H. Kim, J. M. Oh, J. H. No, Y. J. Bang, Y. S. Juhnn, and Y. S. Song, "Involvement of NF- B and AP-1 in COX-2 upregulation by human papillomavirus 16 E5 oncoprotein," *Carcinogenesis*, vol. 30, no. 5, pp. 753–757, 2009.

[60] B. Poligone and A. S. Baldwin, "Positive and negative regulation of NF-κB by COX-2," *Journal of Biological Chemistry*, vol. 276, no. 42, pp. 38658–38664, 2001.

[61] J. L. Liggett, X. Zhang, T. E. Eling, and S. J. Baek, "Anti-tumor activity of non-steroidal anti-inflammatory drugs: Cyclooxygenase- independent targets," *Cancer Letters*, vol. 346, no. 2, pp. 217–224, 2014.

[62] L. C. Chang, L. T. Tsao, C. S. Chang et al., "Inhibition of nitric oxide production by the carbazole compound LCY-2-CHO via blockade of activator protein-1 and CCAAT/enhancer-binding protein activation in microglia," *Biochemical Pharmacology*, vol. 76, no. 4, pp. 507–519, 2008.

[63] B. Kaminska, "MAPK signalling pathways as molecular targets for anti-inflammatory therapy– from molecular mechanisms to therapeutic benefits," *Biochimica et Biophysica Acta (BBA) - Proteins and Proteomics*, vol. 1754, no. 1–2, pp. 253–262, 2005.

[64] P. P. Tak and G. S. Firestein, "NF-κB: a key role in inflammatory diseases," *The Journal of Clinical Investigation*, vol. 107, no. 1, pp. 7–11, 2001.

[65] C. Franceschi and J. Campisi, "Chronic inflammation (inflammaging) and its potential contribution to age-associated diseases," *The Journals of Gerontology Series A: Biological Sciences and Medical Sciences*, vol. 69, no. S1, pp. S4–S9, 2014.